International Journal of Technical Innovation in Modern Engineering & Science (IJTIMES)
Impact Factor: 5.22 (SJIF-2017), e-ISSN: 2455-2585
Volume 4, Issue 6, June-2018

# DESIGN OF MULTI CONTACT–AIDED CELLULAR COMPLIANT MECHANISMS FOR STRESS RELIEF

Adapa Anil Kumar[1], Mrs.Ch.Vasanthalakshmi[2], Mrs.K.Aravinda[3] , Mr.D.J.Johnson[4]
[1]*M.Tech Student (CAD/CAM),Dept. Of ME, Pragati Engineering College, Surampalem, aniladapa93@gmail.com*
[2] *Associate Professor , Dept. Of ME, Pragati Engineering College, Surampalem, vasanthalakshmi.ch@pragati.ac.in*
[3]*Assistant Professor, Dept ,of ME, Pragati Engineering College, Surampalem, aravinda301@gmail.com*
[4]*Assistant Professor, Dept, of ME, Pragati Engineering College, Surampalem, d.jasperjohnson@gmail.com*

***Abstract*— Many engineering applications need materials having specific properties. Some of these applications demand conflicting properties such as high strain – high strength, high strength – low density, high thermal conductivity – high thermal diffusivity. Nature, on the contrary, offers materials of only a limited range of properties. Such materials may not be the most suitable in many cases. Therefore, new materials such as alloys, composites, foams, and/or sandwich structures are tailored to meet specific needs.**

**In this particular study the behaviour of multi contact-aided cellular complaint mechanisms are studied using Finite Element methods , the load carrying capacity of cellular members with multi contact-aided compliant mechanisms is studied under all compression, tension and shearing conditions**.

***Keywords*— Cellular Compliant Mechanisms, Acrylic, HDPE, Polystyrene, Catia V5, Ansys 16.1.**

## I. INTRODUCTION

Cellular structures are either repeated in space in a patterned manner or distributed randomly (as in the case of foams). A unit cell is the representative element of a patterned cellular structure. The unit cell has same effective properties as those of the corresponding extended cellular structure . Many such cellular structures and unit cells are compliant mechanisms. Such that cellular structures can have a relatively high strength-to-weight ratio [1], vibration absorption characteristics [2], and high flexibility [3,4]. New cellular structures such as chiral [5], flex-core [6], and accordion [7] have been developed for their potential applications in daily use. Topology optimization is a tool that can be used to find the features such as the number, location and shape of holes in a solid structure and the distribution of material over a domain. The optimal material distribution depends on specific objectives such as the compliance of a structure for a given volume fraction. Another objective function might involve finding an optimal material microstructure, a process known as inverse homogenization [8]. Homogenization involves estimating effective elastic properties for a given material microstructure. Estimation of homogenized coefficients using finite element (FE) methods was first presented in Ref. [9]. Such homogenization theory has been successfully used to design material microstructures either for a prescribed elasticity matrix and to obtain a composite structure with external properties .The Contact-aided compliant mechanisms, which experience contact during deformation, have also been synthesized using topology optimization . In one such study, unilateral contact is considered for the compliance minimization of structures .

## II. METHODS

### 2. Method

Two alternative approaches are presented for designing complaint structures with graded stiffness. The first approach is focused on achieving graded or increasing stiffness with applied load. The second approach is focused on customizing stiffness according to location.

### 2.1 Design Approach for Graded Stiffness with Applied Load

The purpose of this approach is to design compliant cellular structures with structural elastic stiffness that varies with the magnitude of applied load. Typically, the structures are designed for relatively low effective elastic stiffness under initial loading. Then, they are designed to stiffen as the magnitude of the applied load increases and to exhibit resiliency under a specified range of quasi-static loads by returning to their original form as the applied load is released. The strategy for achieving low effective elastic stiffness is to identify cellular topologies that subject cell walls to transverse loads and elastic bending rather than axial loads and deformation, for which the structures tend to be stiffer. The strategy for increasing the effective elastic stiffness as the magnitude of the load increases is to initiate contact in the cell walls which stiffens the structure and prevents significant additional cell wall bending and yielding.

As documented in Figure 3, the method begins by identifying a compliant cellular topology as a base design (*Step 1*). In this paper, the staggered cell configuration illustrated in Figure 2 is selected to demonstrate the approach. The next step (*Step 2*) is to define a unit cell of the topology as the simplest periodically repeating unit of the material. For geometric feasibility of this basic design, it is essential that cells in an individual row have the same height and cells in an individual column have the same width. In this case, however, we have considered a fully periodically repeating material, and therefore the cell size is uniform throughout the specimen. Independently varying the width of each column and the height of each row would increase the number of design variables required to define the structure, but the design method would remain the same

### 2.2 Design Approach for Graded Stiffness with Location

The previous approach is efficient when the geometry is periodically repeated. However, if the cells and corresponding stiffness are varied with location, the number of design variables increases along with the number of design iterations. The problem becomes more difficult to solve efficiently with contact conditions because each design iteration requires an ANSYS evaluation. In the following approach, a parametric approximate model is constructed for a basic unit cell, based on data from detailed ANSYS analyses. The regression model is utilized in place of expensive ANSYS analyses to enable rapid, computationally efficient design of structures with stiffness that varies with location and/or magnitude of applied load.

The strategy here is to populate a geometric domain with individual spring-like structures with individually customized stiffness profiles. Sample geometries are illustrated in Figure 4, all of which provide variable stiffness with the influence of surface contact. An object, such as a compliant chair pad or vehicle bumper, would be populated with a matrix of these structures, which can be customized to provide targeted force-deflection characteristics for specific applied loads and spatial constraints.

## III. DESIGN

CATIA which stands for Computer Aided Three Dimensional Interactive Application is CAD software owned and developed by Dassault Systems and marketed worldwide by IBM. It is the world's leading CAD/CAM software for design and manufacturing. CATIA supports multiple stages of product development through conceptualization, design, engineering and manufacturing.

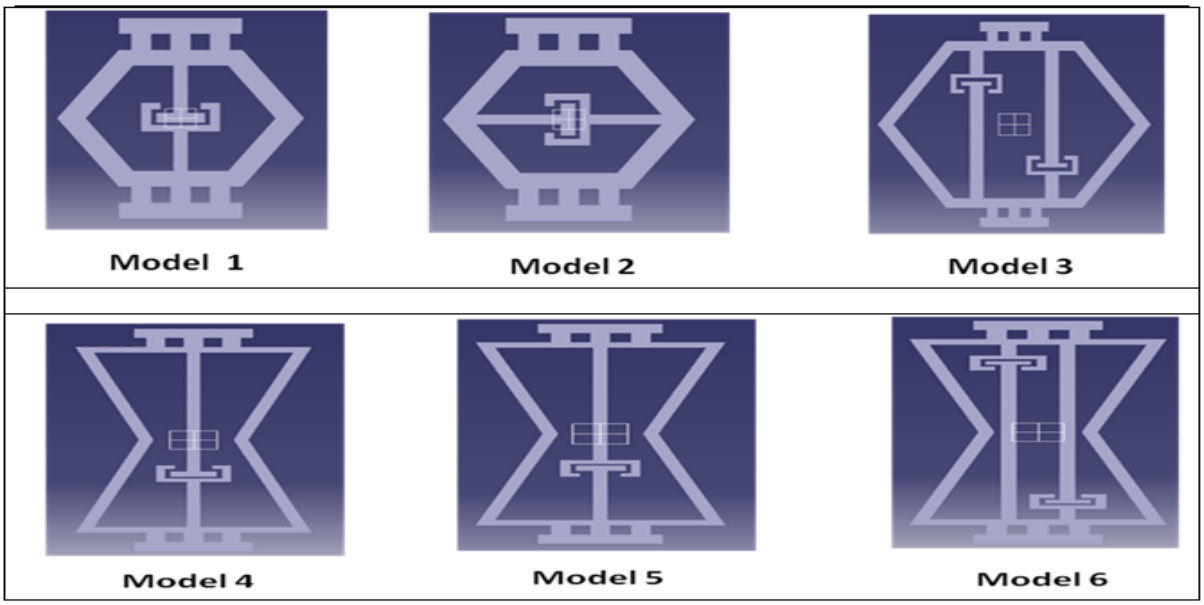

## IV.ANALYSIS

ANSYS is the standard FEA teaching tool within the Mechanical Engineering Department at many colleges. ANSYS is also used in Civil and Electrical Engineering, as well as the Physics and Chemistry departments.

**Static Structural And Model Analysis With Acrylic**

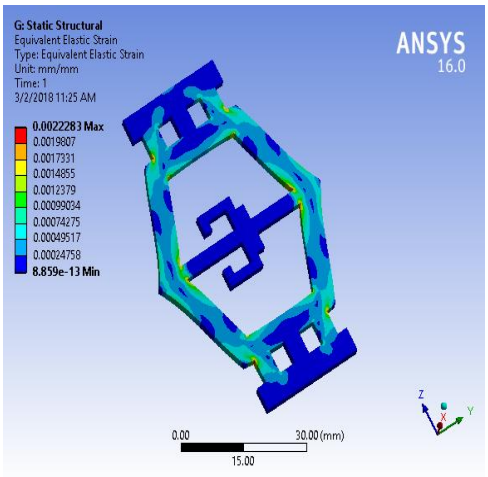


Fig: 1.1 picture showing equivalent strain with acrylic

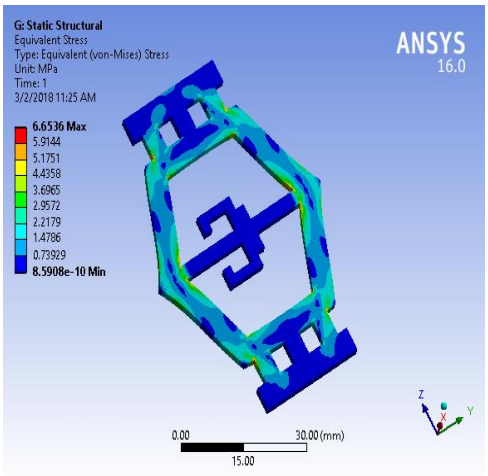


Fig: 1.2 picture showing equivalent stress with acrylic

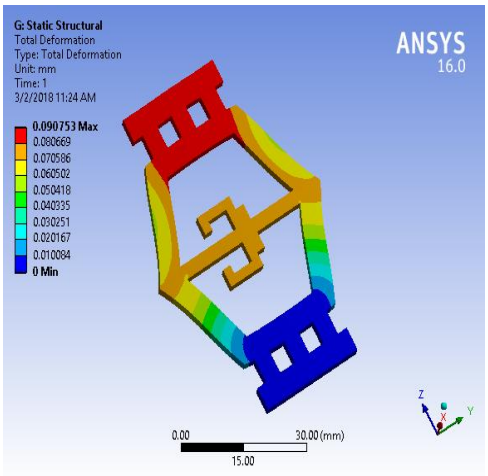


Fig: 1.3 picture showing total deformation with acrylic

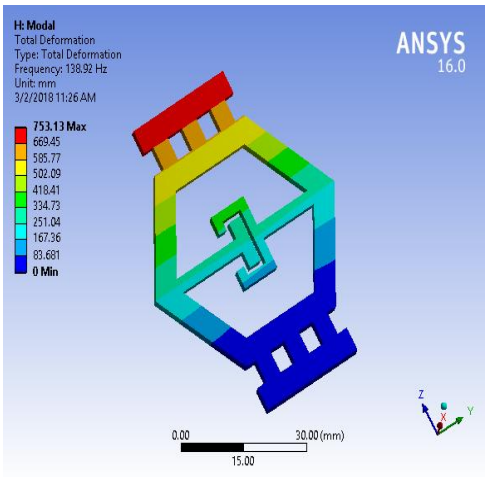


Fig: 1.4 picture showing deformation 1 with acrylic

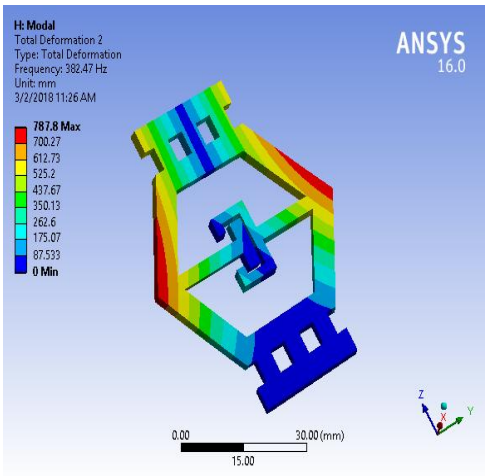


Fig: 1.5 picture showing deformation 2 with acrylic

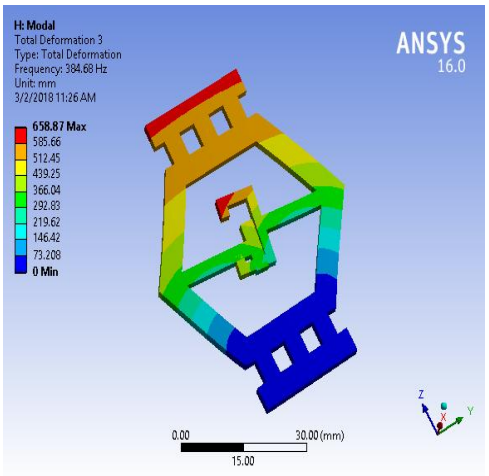


Fig: 1.6 picture showing deformation 3 with acrylic

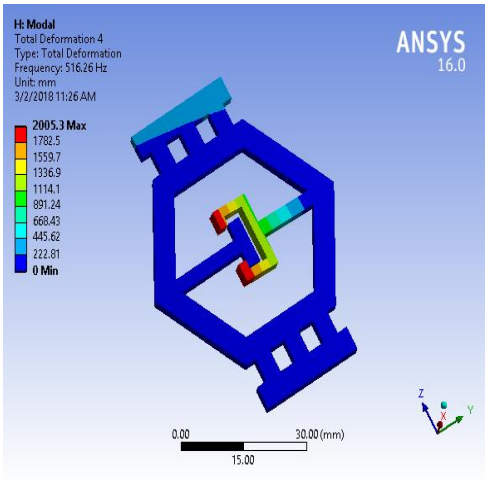


Fig: 1.7 picture showing deformation 4 with acrylic

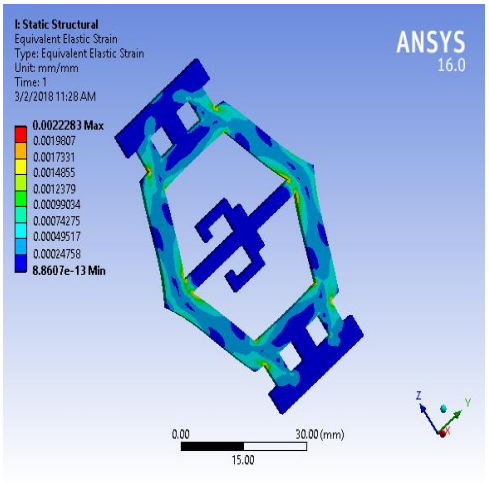


Fig: 2 picture showing equivalent strain with HDPE

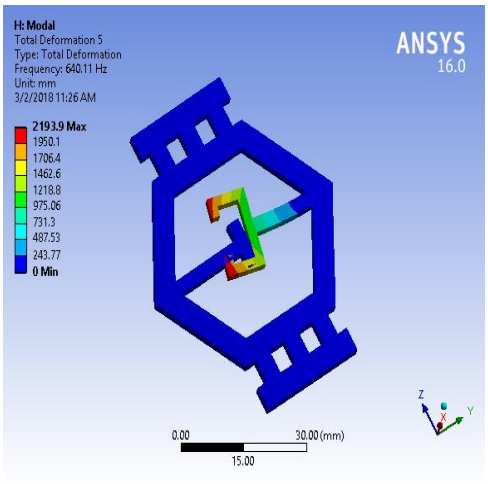


Fig: 1.8 picture showing deformation 5 with acrylic

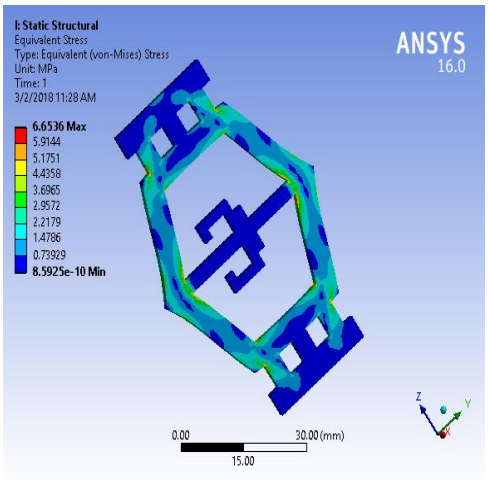


Fig: 2.1 picture showing equivalent stress with HDPE

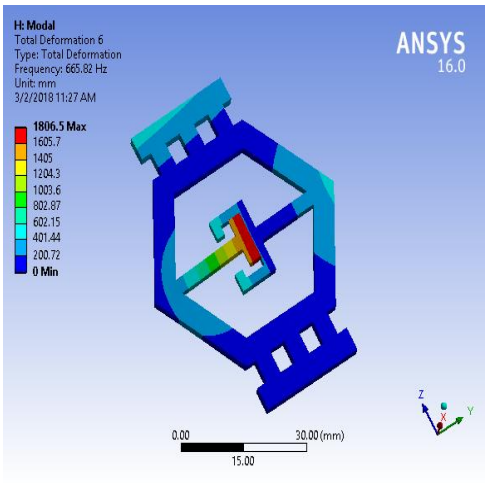


Fig: 1.9 picture showing deformation 6 with acrylic

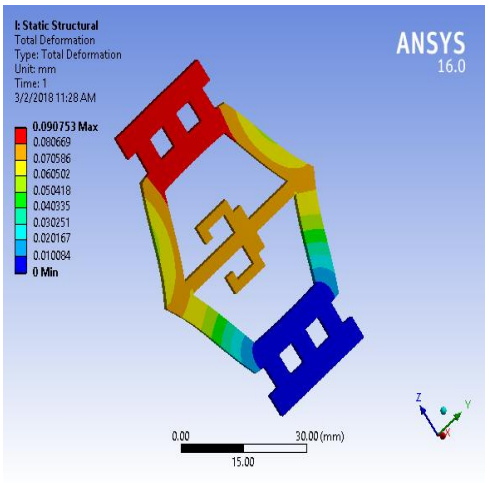


Fig: 2.2 picture showing total deformation with HDPE

**Static structural and model analysis with HDPE**

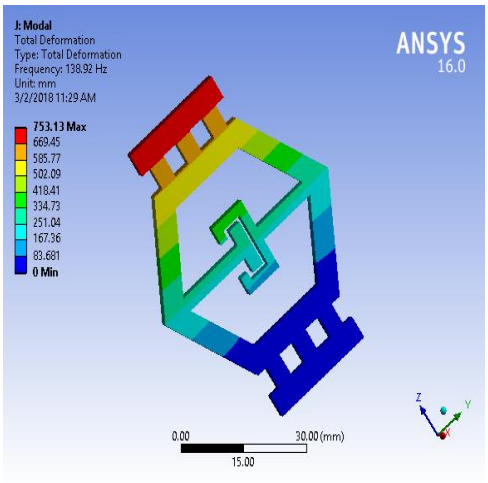


Fig: 2.4 picture showing deformation 1 with HDPE

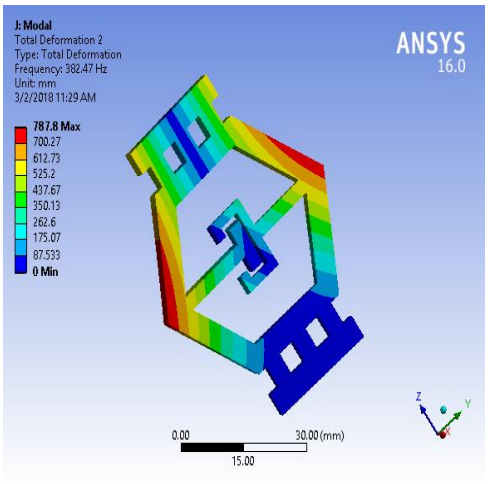


Fig: 2.5 picture showing deformation 2 with HDPE

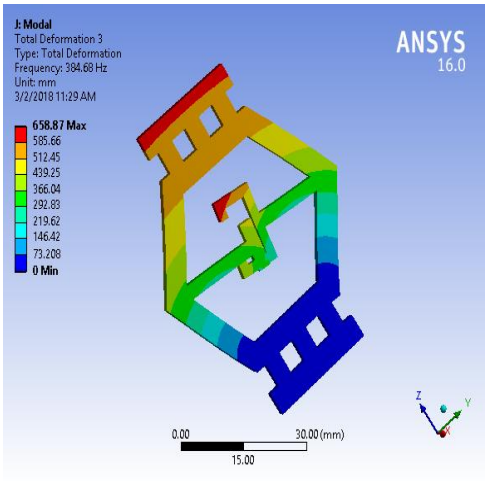


Fig: 2.6 picture showing deformation 3 with HDPE

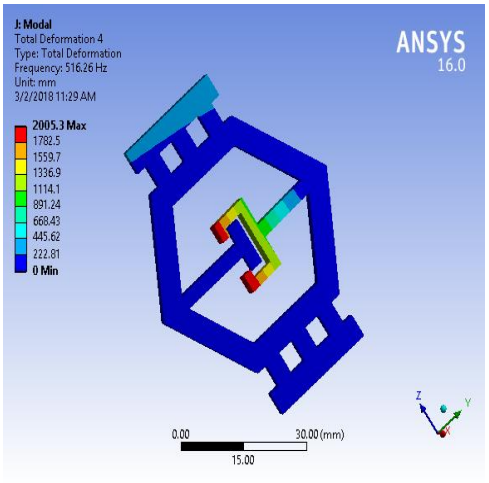


Fig: 2.7 picture showing deformation 4 with HDPE

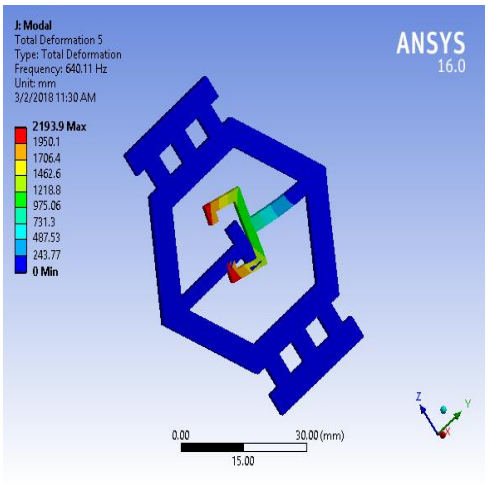


Fig: 2.8 picture showing deformation 5 with HDPE

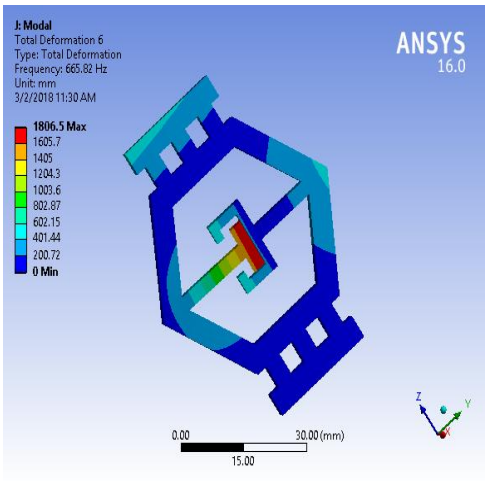


Fig: 2.9 picture showing deformation 6 with HDPE

**Static structural and model analysis of model 2 with polystyrene**

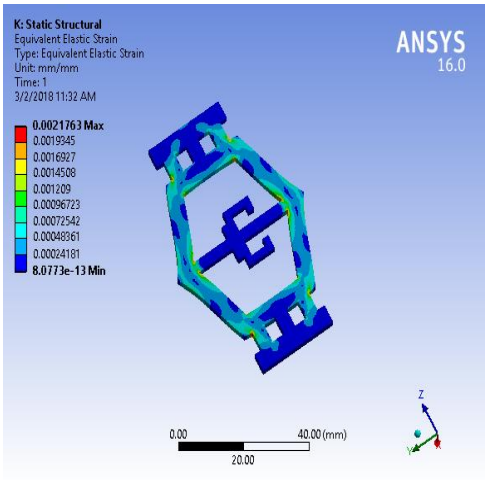


Fig: 3.1 picture showing equivalent strain with polystyrene

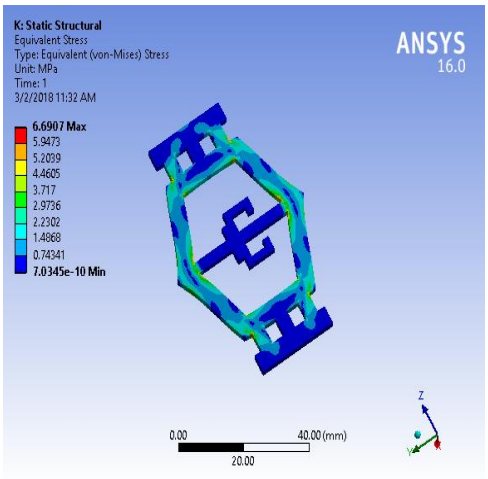


Fig:3.2 picture showing equivalent stress with polystyrene

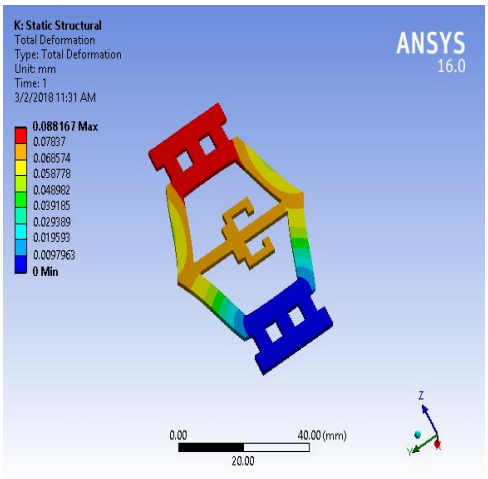


Fig: 3.3 picture showing total deformation with polystyrene

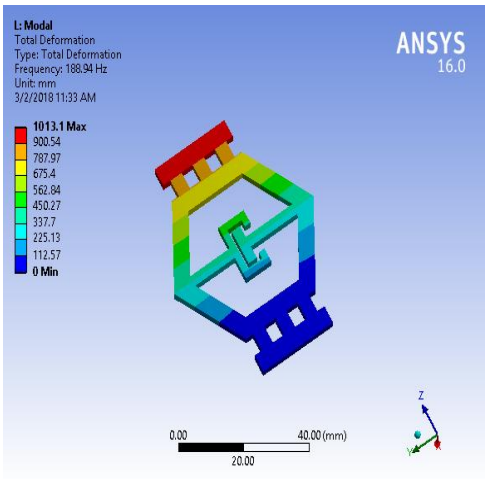


Fig: 3.4 picture showing deformation 1 with polystyrene

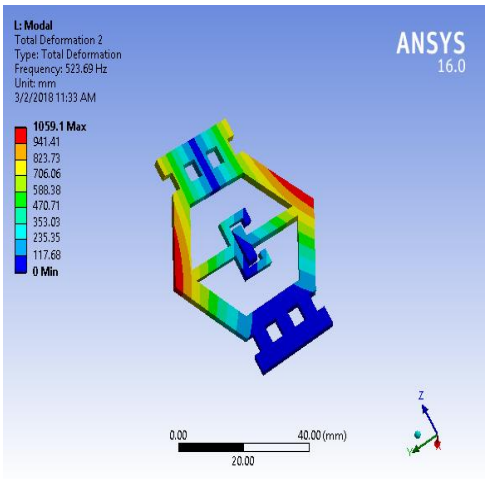


Fig: 3.5 picture showing deformation 2 with polystyrene

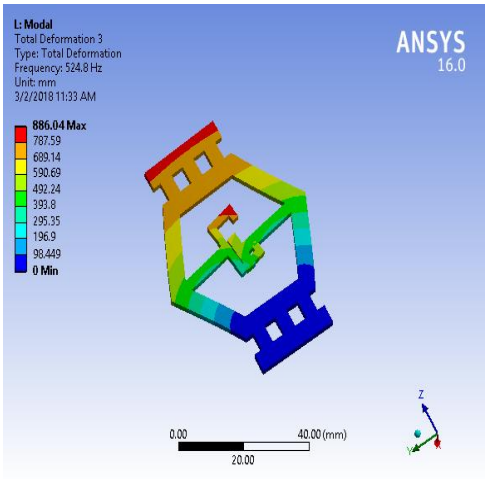


Fig: 3.6 picture showing deformation 3 with polystyrene

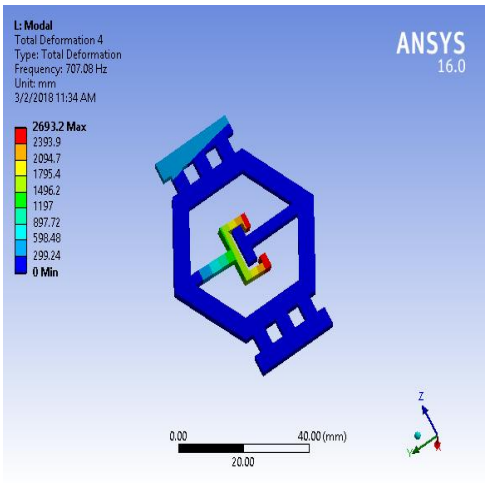


Fig: 3.7 picture showing deformation 4 with polystyrene

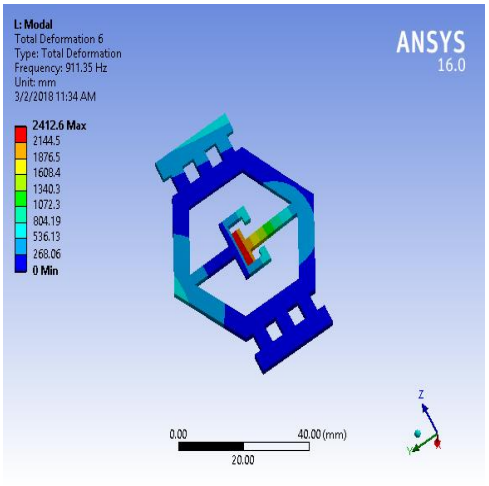


Fig: 3.9 picture showing deformation 6 with polystyrene

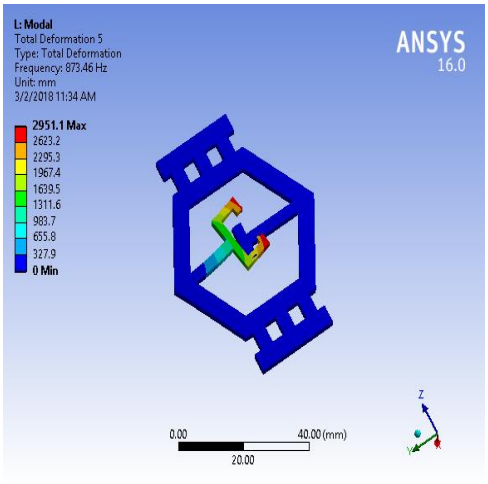


Fig: 3.8 picture showing deformation 5 with polystyrene

## V . REPORT

**Table 1 static structural and model analysis of different models with acrylic**

| Acrylic | equivalent strain (mm/mm) | | equivalent stress (Mpa) | | total deformation (mm) | |
|---|---|---|---|---|---|---|
| | min | max | min | max | min | max |
| model 1 | 1.01E-12 | 0.003482 | 6.68E-10 | 11.372 | 0.011014 | 0.099126 |
| model 2 | 8.86E-13 | 0.002228 | 8.59E-10 | 6.6536 | 0.010084 | 0.090753 |
| model 3 | 2.34E-12 | 0.004028 | 1.38E-09 | 12.969 | 0.10752 | 0.96772 |
| model 4 | 2.45E-12 | 0.004015 | 1.06E-09 | 13.181 | 0.086619 | 0.77957 |
| model 5 | 1.32E-15 | 0.005605 | 5.37E-13 | 17.852 | 0.11562 | 1.0406 |
| model 6 | 1.06E-16 | 0.005604 | 8.91E-14 | 17.904 | 0.11656 | 1.049 |

**Graphs**

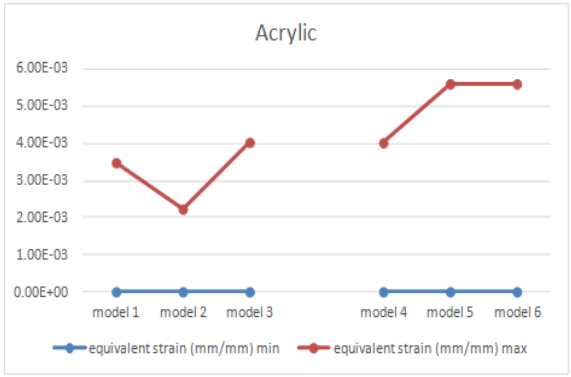


Fig: 5.1 graph showing equivalent strain with acrylic

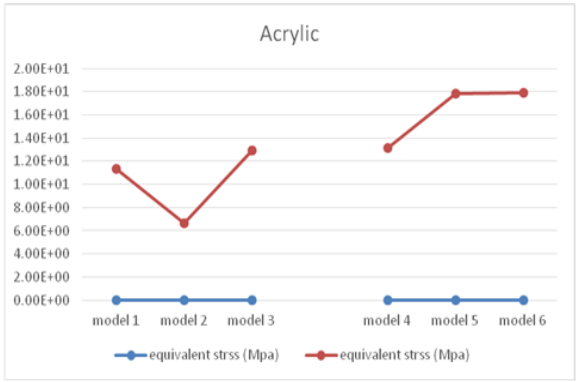


Fig: 5.2 graph showing equivalent stress with acrylic

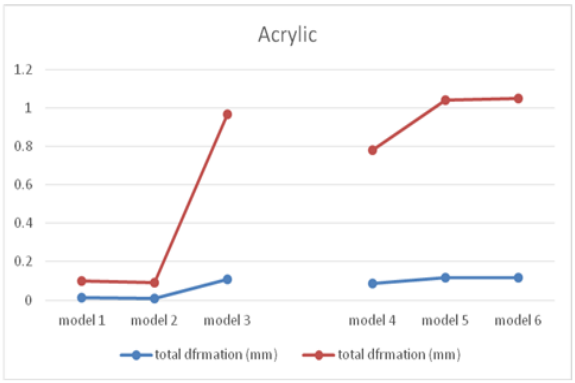


Fig: 5.3 graph showing total deformation with acrylic

**Table 2 static structural and model analysis of different models with HDPE**

| HDPE | equivalent strain (mm/mm) | | equivalent stress (Mpa) | | total deformation (mm) | |
|---|---|---|---|---|---|---|
| | min | max | min | max | min | Max |
| model 1 | 1.85E-12 | 0.008828 | 4.90E-10 | 11.348 | 0.027932 | 0.25139 |
| model 2 | 8.86E-13 | 0.002228 | 8.59E-10 | 6.6536 | 0.010084 | 0.090753 |
| model 3 | 5.12E-12 | 0.01022 | 1.38E-09 | 12.945 | 0.27223 | 2.4501 |
| model 4 | 4.40E-12 | 0.010165 | 7.80E-10 | 13.173 | 0.21977 | 1.9779 |
| model 5 | 2.09E-15 | 0.014197 | 1.39E-12 | 17.868 | 0.29342 | 2.6407 |
| model 6 | 2.71E-16 | 0.014195 | 1.40E-13 | 17.922 | 0.29587 | 2.6629 |

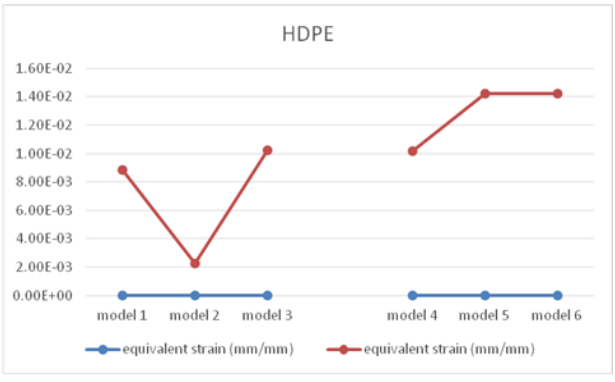


Fig: 5.4 graph showing equivalent strain with HDPE

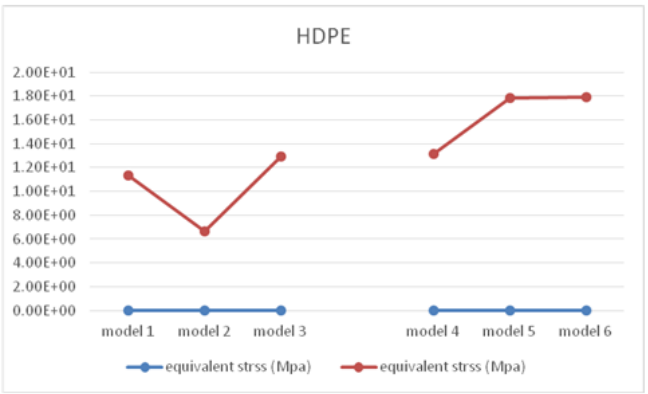


Fig: 5.5 graph showing equivalent stress with HDPE

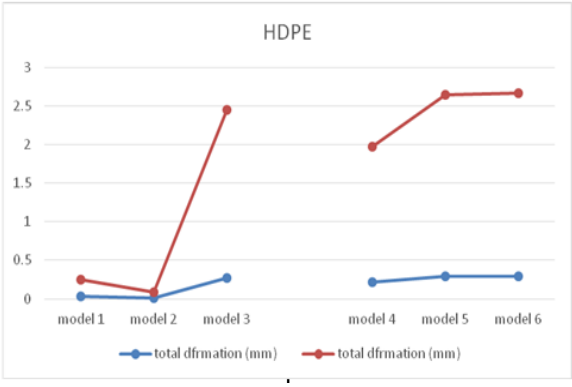


Fig: 5.6 graph showing total deformation with HDPE

**Table 3 static structural and model analysis of different models with polystyrene**

| Polystyrene | equivalent strain (mm/mm) | | equivalent stress (Mpa) | | total deformation (mm) | |
|---|---|---|---|---|---|---|
| | min | max | min | max | min | max |
| model 1 | 8.17E-13 | 0.003385 | 7.38E-10 | 11.398 | 0.010698 | 0.096283 |
| model 2 | 8.08E-13 | 0.002176 | 7.03E-10 | 6.6907 | 0.009796 | 0.088167 |
| model 3 | 2.33E-12 | 0.003912 | 1.29E-09 | 12.994 | 0.10459 | 0.94132 |
| model 4 | 1.80E-12 | 0.003924 | 1.64E-09 | 13.189 | 0.084109 | 0.75698 |
| model 5 | 2.29E-15 | 0.005453 | 9.21E-13 | 17.836 | 0.11225 | 1.0102 |
| model 6 | 1.23E-16 | 0.005452 | 9.64E-14 | 17.886 | 0.11313 | 1.0181 |

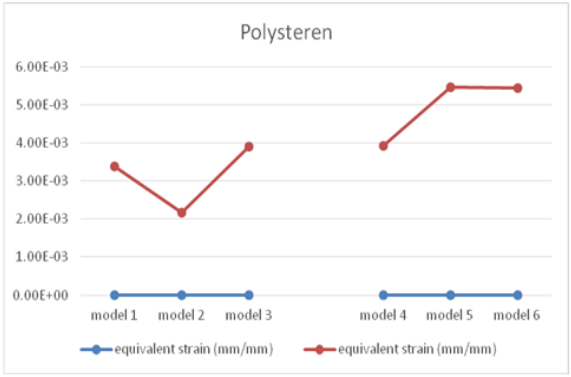


Fig: 5.7 graph showing equivalent strain with polystyrene

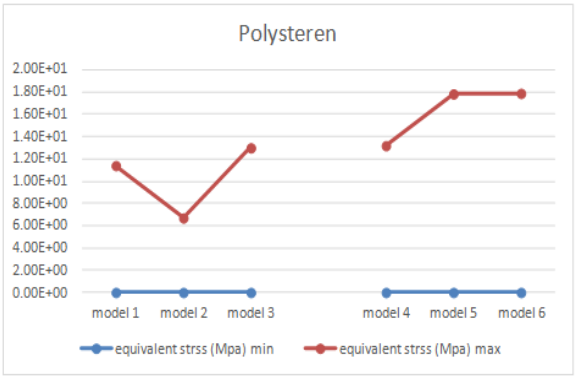


Fig: 5.8 graph showing equivalent stress with polystyrene

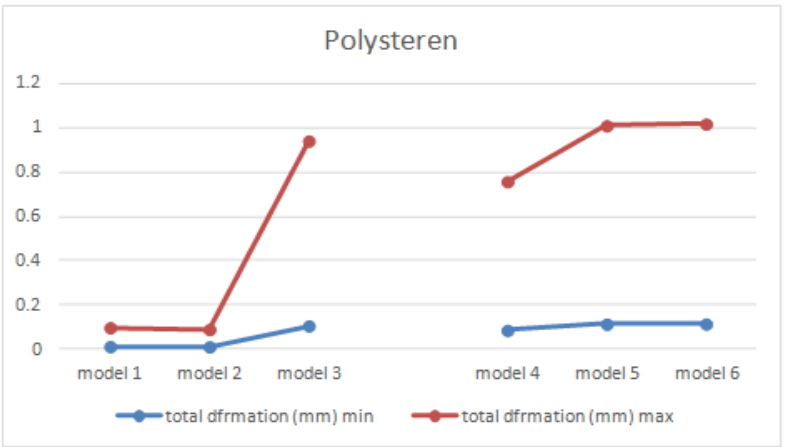


Fig: 3.8 picture showing deformation 5 with polystyrene

**Table 4 Natural frequencies of different models with acrylic**

| Acrylic | Natural frequency mode 1 (Hz) | Natural frequency mode 2 (Hz) | Natural frequency mode 3 (Hz) | Natural frequency mode 4 (Hz) | Natural frequency mode 5 (Hz) | Natural frequency mode 6 (Hz) |
|---|---|---|---|---|---|---|
| model 1 | 139..5 | 389.79 | 398.73 | 569.37 | 656.63 | 749.27 |
| model 2 | 138.92 | 382.47 | 384.68 | 516.26 | 640.11 | 665.82 |
| model 3 | 54.549 | 80.807 | 131.62 | 159.85 | 199.05 | 203.59 |
| model 4 | 46.574 | 50.992 | 98.416 | 121.43 | 131.82 | 282.83 |
| model 5 | 46.053 | 52.021 | 70.784 | 105.51 | 116.66 | 273.3 |
| model 6 | 43.615 | 48.513 | 58.55 | 72.508 | 78.795 | 85.704 |

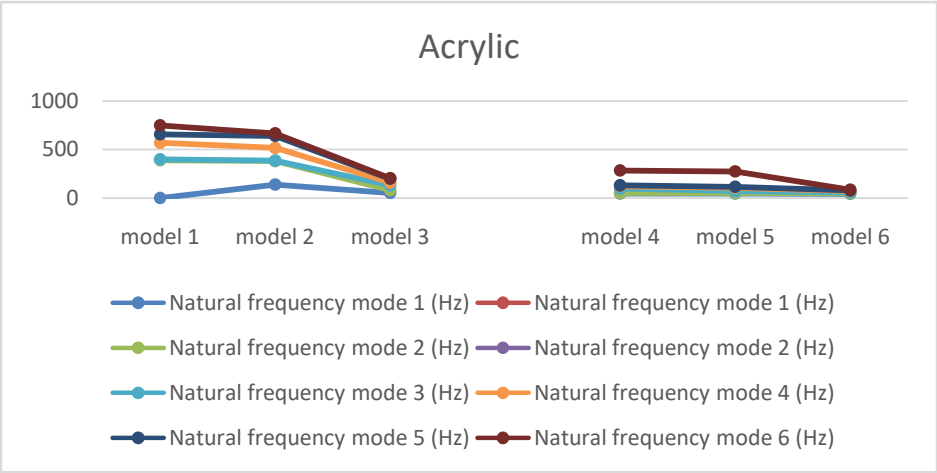


Fig: 5.10 graph showing natural frequencies with acrylic

**Table 5 Natural frequencies of different models with HDPE**

| HDPE | Natural frequency mode 1 (Hz) | Natural frequency mode 2 (Hz) | Natural frequency mode 3 (Hz) | Natural frequency mode 4 (Hz) | Natural frequency mode 5 (Hz) | Natural frequency mode 6 (Hz) |
|---|---|---|---|---|---|---|
| model 1 | 127.17 | 305.43 | 312.01 | 448.39 | 509.63 | 575.66 |
| model 2 | 138.92 | 382.47 | 384.68 | 516.26 | 640.11 | 665.82 |
| model 3 | 49.091 | 65.975 | 102.98 | 125.5 | 153.81 | 156.11 |
| model 4 | 47.376 | 47.915 | 81.129 | 95.459 | 107.93 | 233.05 |
| model 5 | 45.881 | 49.291 | 63.271 | 84.914 | 99.498 | 238.93 |
| model 6 | 41.299 | 44.978 | 54.146 | 56.288 | 60.506 | 70.388 |

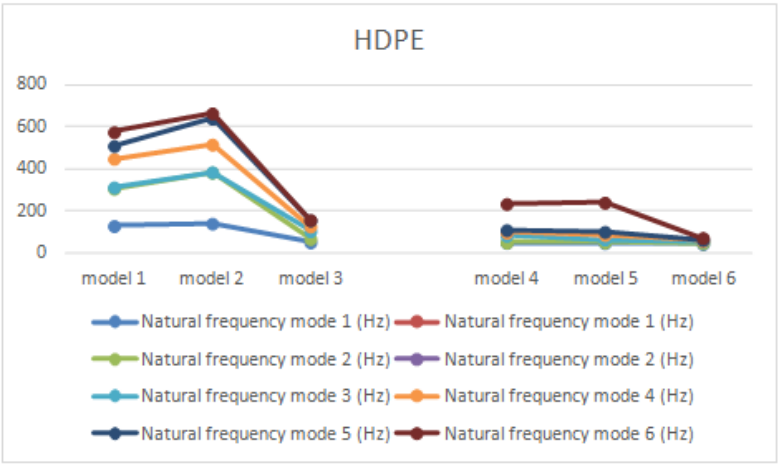


Fig: 5.11 graph showing natural frequencies with HDPE

**Table 6 Natural frequencies of different models with polystyrene**

| Polystyrene | Natural frequency mode 1 (Hz) | Natural frequency mode 2 (Hz) | Natural frequency mode 3 (Hz) | Natural frequency mode 4 (Hz) | Natural frequency mode 5 (Hz) | Natural frequency mode 6 (Hz) |
|---|---|---|---|---|---|---|
| model 1 | 189.71 | 531.77 | 545.97 | 777.59 | 900.4 | 1022.4 |
| model 2 | 188.94 | 523.69 | 524.8 | 707.08 | 873.46 | 911.35 |
| model 3 | 74.403 | 110.12 | 180.18 | 218.9 | 271.52 | 278.55 |
| model 4 | 63.233 | 69.255 | 134.6 | 165.66 | 181.2 | 385.48 |
| model 5 | 62.431 | 70.62 | 96.565 | 143.91 | 160.06 | 372.87 |
| model 6 | 59.165 | 65.878 | 79.82 | 99.019 | 107.56 | 116.86 |

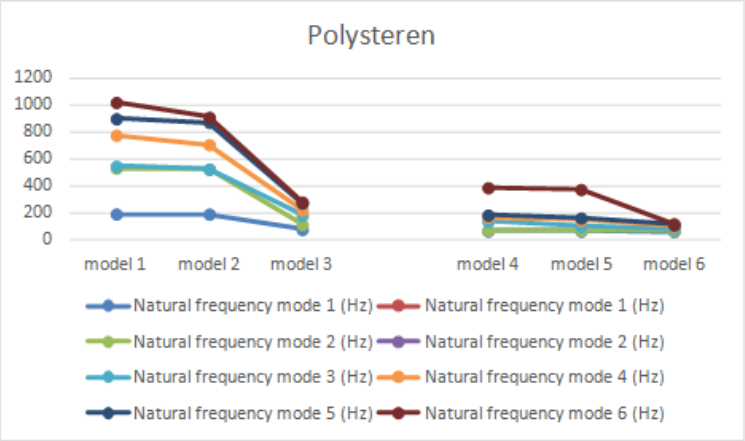


Fig: 5.12 graph showing natural frequencies with polysteren

## VI. RESULTS AND DISCUSSIONS

Here we are conducting experimentation to study the behavior of compliance cellular mechanism with respect to the arrangement of web, these webs are use full for adding additional stiffness to the cells under loaded conditions, and basically these webs play a major role in modifying the structural behavior of the cells. Here we studied six different models of compliance cellular mechanism

In first two models the orientation of the web is changed, first model has its web oriented in the direction of loading and the second model has its web at 90 degrees to the direction of loading. Here the stress strains and deformations have reduced significantly when we the orientation of the web is 90 degrees to the direction of loading. In third model overall dimensions are doubled to accommodate two webs in opposite orientation aligned in the direction of loading, in this case though the geometry is doubled the deformations are reduced astonishingly. Here the stiffness is due to double web, from these observations we can state that incorporating multiple webs in cells will further increase the stiffness of the cell.

These observations are entirely related to honeycombed shaped compliance cellular mechanisms, similar study is not carried with the rectangular cells because web at 90 degrees is not possible in rectangular cells but incorporations of multiple webs will surely add more stiffness to the cells. Similar trends are followed by specimens made by all materials.

## VII . CONCLUSIONS

This study is mainly concentrated on the behavior of the compliance cellular structures with varying configurations of stiffeners. Compliance cellular mechanisms play a very crucial role in modern sciences, they find their applications in aerospace bionics and robotics etc, in this work two different geometries of cells are studied with three different configurations of the stiffeners, three different materials are also compared, the following observations are made from the simulation study.

1. From the observations inverting the compliance mechanism will reduce the deformations and stress considerably
2. Same phenomenon is repeated in both hexagonal and rectangular cellular models
3. Incorporating multiple stiffeners is of no use according to the simulations, stress and deformations are increasing in this case
4. Comparing the materials has yielded a different result acrylic and polystyrene reported similar behavior while HDPE showed little poor qualities.
5. Comparing the cellular geometry hexagonal cell have higher stiffness and strength when compared with rectangular cell made with same material.

## References

[1] Gibson, L. J., and Ashby, M. F., 1997, Cellular Solids—Structure and Proper- ties, 2nd ed., Cambridgedge University Press, Cambridge.

[2] Scarpa, F., and Tomlinson, G., 1999, "Theoretical Characteristics of the Vibration of Sandwich Plates With Inplane Negative Poisson's Ratio Values," J. Sound Vib., 230(1), pp. 45–67.

[3] Scarpa, F., Panayiotou, P., and Tomlinson, G., 2000, "Numerical and Experimental Uni-axial Loading on In-Plane Auxetic Honeycombs," J. Strain Anal., 35(5), pp. 383–388.

[4] Olympio, K. R., and Gandhi, F., 2009, "Flexible Skins for Morphing Aircraft Using Cellular Honeycomb Cores," J. Intell. Mater. Syst. Struct., 21(17), pp. 1–17.

[5] Bornengo, D., Scarpa, F., and Remillat, C., 2005, "Evaluation of Hexagonal Chiral Structure for Morphing Airfoil Concept," Proc. Inst. Mech. Eng., Part G: J. Aerosp. Eng., 219(3), pp. 185–192.

[6] Henry, C., and McKnight, G., 2006, "Cellular Variable Stiffness Materials for Ultra-Large Reversible Deformations in Reconfigurable Structures," Proc. SPIE, 6170, pp. 1–12.

[7] Olympio, K. R., and Gandhi, F., 2009, "Zero Poisson's Ratio Cellular Honey- combs for Flex Skins Undergoing One Dimensional Morphing," J. Intell. Mater. Syst. Struct., 21(11), pp. 1–17

.[8] Mehta, V., Frecker, M., and Lesieutre, G. A., 2009, "Stress Relief in Contact- Aided Compliant Cellular Mechanisms," ASME J. Mech. Des., 31(9), pp. 1–11.

[9] BENDSOE, M. P., AND SIGMUND, O., 2003, TOPOLOGY OPTIMIZATION THEORY, METHODS AND APPLICATIONS, SPRIGER GERMANY.